Application of Hybrid FEM to Heat Transfer of Skin Tissues

Yi Xiao

Research School of Engineering, Australian National University, Acton, ACT 2601, Australia

ABSTRACT

This paper presents an overview on applications of hybrid finite element method (FEM) to heat transfer analysis of skin tissue materials. Recent developments on the hybrid fundamental solution based FEM of heat transfer in skin tissues are described. Formulations for all cases are derived by means of modified variational functional and fundamental solutions. Generation of elemental stiffness equations from the modified variational principle is also discussed. Finally, a brief summary of the approach and potential research topics is provided.

Keywords: Finite Element Method, Fundamental Solution, Skin Tissues.

I. INTRODUCTION

Heat transfer in skin tissues and biomaterials has been widely investigated [1-4]. It should be mentioned that analytical solutions which are available only for a few problems with simple geometries and boundary conditions [5-17]. Therefore, development of efficient numerical methods is vital for solving engineering problems [18-24]. The first is the so-called hybrid Trefftz FEM (or T-Trefftz method) [25, 26]. Unlike in the conventional FEM, the T-Trefftz method couples the advantages of conventional FEM [27-30] and BEM [31-33]. In contrast to the standard FEM, the T-Trefftz method is based on a hybrid method which includes the use of an independent auxiliary inter-element frame field defined on each element boundary and an independent internal field chosen so as to a prior satisfy the homogeneous governing differential equations by means of a suitable truncated T-complete function set of homogeneous solutions. Since 1970s, T-Trefftz model has been considerably improved and has now become a highly efficient computational tool for the solution of complex boundary value problems. It has been applied to potential problems [4, 34-36], two-dimensional elastics [37, 38], elastoplasticity [39, 40], fracture mechanics [41-43], micromechanics analysis [44, 45], problem with holes [46, 47], heat conduction [48-50], thin plate bending [51-54], thick or moderately thick plates [55-59], three-dimensional problems [60], piezoelectric materials [61-65], and contact problems [66-68].

On the other hand, the hybrid FEM based on the fundamental solution (F-Trefftz method for short) was initiated in 2008 [26, 69] and has now become a very popular and powerful computational methods in mechanical engineering. The F-Trefftz method is significantly different from the T-Trefftz method discussed above. In this method, a linear combination of the fundamental solution at different points is used to approximate the field variable within the element. The independent frame field defined along the element boundary and the newly developed variational functional are employed to guarantee the inter-element continuity, generate the final stiffness equation and establish linkage between the boundary frame field and internal field in the element. This review will focus on the F-Trefftz finite element method.

The F-Trefftz finite element method, newly developed recently [26, 69], has gradually become popular in the field of mechanical and physical engineering since it is initiated in 2008 [26, 70, 71]. It has been applied to potential problems [36, 72-74], plane elasticity [38, 75, 76], composites [77-81], piezoelectric materials [82-84], three-dimensional problems [85], functionally graded

materials [86-88], bioheat transfer problems [89-95], thermal elastic problems [96], hole problems [97, 98], heat conduction problems [69, 99], micromechanics problems [44, 45], and anisotropic elastic problems [100-102].

Following this introduction, the present review consists of 3 sections. F-Trefftz FEM for nonlinear heat transfer in FGMs is described in Section 2. It describes in detail the method of deriving element stiffness equations. Section 3 focuses on the essentials of F-Trefftz elements for composites. Finally, a brief summary of the developments of the Treffz methods is provided.

II. Heat Transfer in Multi-Layer Skin Tissues

2.1 Basic Equations
Consider

In biological engineering, the human skin tissue is usually modeled as a three layered material including the epidermis, the dermis and the subcutaneous fat layer. Besides, an inner tissue which is the region from the inner surface of the subcutaneous fat layer to the core of the skin is also introduced [103]. In the four layered biological model shown in Figure 1, each layer is supposed to be homogeneous. within which the blood perfusion, thermal conductivity, and heat capacity are assumed to be constant.
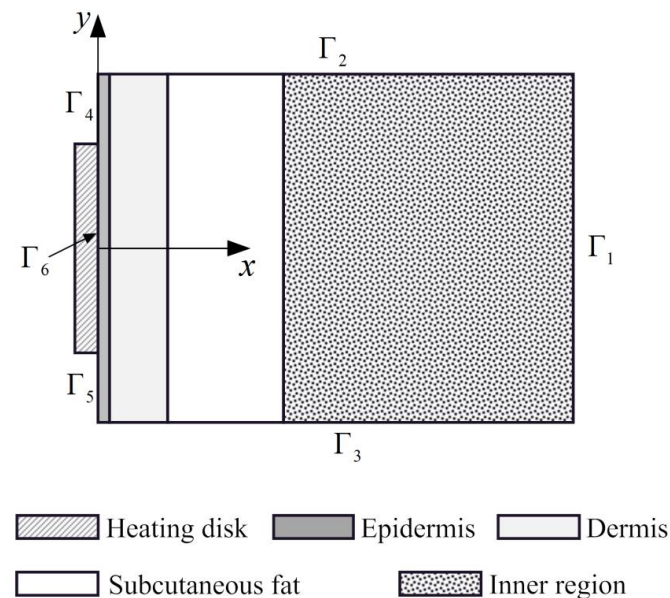

Figure 1. Diagram of the multi-layer skin tissues

The steady-state heat transfer in the biological tissue is governed by the well-known Pennes bioheat equation

$$k\nabla^2 T + \rho_b c_b \omega_b (T_b - T) + Q_r + Q_m = 0 \qquad (1)$$

where k is the thermal conductivity, T is the temperature change of the tissue, ∇^2 is the Laplace operator, ρ_b, c_b and ω_b are respectively the density, specific heat and perfusion rate of blood, T_b is the temperature of arterial blood, Q_m and Q_r are metabolic heat generation and heat deposition in the tissue caused by outer heating factor such as laser, microwave, respectively.

The bioheat transfer equation (1) is a statement of the law of conservation of energy. The first term on the left hand-side of Eq (1) represents the heat conduction in the tissue caused by the temperature gradient, and the second term stands for heat transport between the tissue and microcirculatory blood perfusion. The third and last terms are internal heat generation due to tissue metabolism and outer heating sources.

In this section, a contact heat source, i.e. a heating disk as displayed in Figure 1, is considered to represent the potential outer burning injury and investigate the induced temperature variation in the multi-layer skin tissue under different heating temperature. In our analysis the assumption that no interfacial resistance exists between the heating source and the skin surface is employed. Therefore, the temperature at the skin surface which is in contact with the heating disk remains constant during heating. Besides, the temperature change caused by the heating disk is much greater than the metabolic heat generation, so the metabolic heat generation is negligible here [104]. Simultaneously, the internal heat generation caused by outer heating source is also neglected. As a result, the bioheat equation (1) reduces to

$$k\nabla^2 T + \rho_b c_b \omega_b (T_b - T) = 0 \qquad (2)$$

Specially, when the blood perfusion rate is zero, this is the fact that no blood flow exists in the epidermis layer, then the governing equation (2) reduces to the standard Laplace equation

$$k\nabla^2 T = 0 \qquad (3)$$

In the bioheat transfer model under consideration, the boundary Γ_1 represents the bottom-most surface of the skin, thus we assume the temperature on it is equivalent to the body core temperature T_c, that is

$$T = T_c \quad \text{at boundary } \Gamma_1 \qquad (4)$$

At the upper and bottom surfaces, no heat flow runs into the skin tissue along these two edges by assuming that the tissue far from the area of interest is not affected by the imposed thermal disturbance, so the adjacent condition is given

$$-k\frac{\partial T}{\partial n} = 0 \quad \text{at boundaries } \Gamma_2 \text{ and } \Gamma_3 \qquad (5)$$

The part of the epidermis surface is directly exposed to the environmental fluid, so the heat exchange occurs between the environmental fluid and skin via convection and radiation. Because, in biological tissues, the effect of radiation from the surrounding is very small in contrast to the convection, so the radiation is neglected here [89]. Also, the cooling of the human skin by the evaporation of sweat should be considered since the heat loss due to evaporation has been found to contribute approximately 15% of the total heat loss from the skin surface [104]. Thus, we have

$$-k\frac{\partial T}{\partial n} = h_\infty\left(T - T_\infty\right) + E_s \quad \text{at } \Gamma_4 \text{ and } \Gamma_5 \qquad (6)$$

where h_∞ and T_∞ are respectively the ambient convection coefficient and temperature, E_s is the heat loss due to sweat evaporation on the skin surface.

Finally, at the boundary where the heating disk is applied, the temperature is assumed to be equal to the temperature of heating disk T_d, i.e.

$$T = T_d \qquad \text{at } \Gamma_6 \qquad (7)$$

2.2 Dimensionless Form

Due to the significant scale difference of variables in Eq. (1), the dimensionless variables defined as follows are introduced

$$X = \frac{x}{L_0}, \quad Y = \frac{y}{L_0}, \quad \Phi = \frac{(T - T_b)k_0}{Q_0 L_0^2}, \quad K = \frac{k}{k_0} \qquad (8)$$

where L_0 is a reference length of the biological body, k_0, ρ_0, c_0 and Q_0 are respectively reference values of the thermal conductivity, density, specific heat and heat source term.

Making use of the new variables defined by Eq (8), the Laplace operator in Eq (3) becomes

$$\frac{\partial^2 T}{\partial x^2} + \frac{\partial^2 T}{\partial y^2} = \frac{Q_0 L_0^2}{k_0}\frac{1}{L_0^2}\left(\frac{\partial^2 \Phi}{\partial X^2} + \frac{\partial^2 \Phi}{\partial Y^2}\right) \qquad (9)$$

Eq (1) can then be rewritten as follows

$$K\nabla^2\Phi - S_b\Phi + \frac{Q_r + Q_m}{Q_0} = 0 \qquad (10)$$

where

$$S_b = \frac{L_0^2 \rho_b c_b \omega_b}{k_0} \qquad (11)$$

At the same time, the corresponding boundary conditions reduce to

$$\begin{cases} \Phi = \Phi_c & \text{on } \Gamma_1 \\ q = -K\dfrac{\partial \Phi}{\partial n} = 0 & \text{on } \Gamma_2 \text{ and } \Gamma_3 \\ q = -K\dfrac{\partial \Phi}{\partial n} = H_\infty\left(\Phi - \Phi_\infty\right) + \tilde{E}_s & \text{on } \Gamma_4 \text{ and } \Gamma_5 \\ \Phi = \Phi_d & \text{on } \Gamma_6 \end{cases} \qquad (12)$$

where

$$H_\infty = \frac{h_\infty L_0}{k_0}, \quad \tilde{E}_s = \frac{E_s}{Q_0 L_0} \qquad (13)$$

2.3 Hybrid FE Implementation

2.3.1 Variational Functional

In the present hybrid finite element formulation, the hybrid functional associated with two independent fields Φ, $\tilde{\Phi}$ defined inside the element domain and over element boundary respectively are constructed as[19]

$$\Pi_{me} = -\frac{1}{2}\int_{\Omega_e}\left\{K\left[\left(\frac{\partial \Phi}{\partial x_1}\right)^2 + \left(\frac{\partial \Phi}{\partial x_2}\right)^2\right] + S_b\Phi^2\right\}d\Omega \qquad (14)$$

$$-\int_{\Gamma_{qe}}\overline{q}\tilde{\Phi}d\Gamma + \int_{\Gamma_e}q(\tilde{\Phi} - \Phi)d\Gamma - \frac{1}{2}\int_{\Gamma_{ce}}H_\infty\left(\tilde{\Phi} - \Phi_\infty\right)^2 d\Gamma$$

where Γ_{qe} and Γ_{ce} are element boundaries with specified heat flux and convection condition, respectively. Ω_e represents the domain of element e with boundary Γ_e, as shown in Figure 2**Error! Reference source not found.**. Besides, in this figure, Γ_{te} and Γ_{le} stand for respectively the element boundary on which the temperature is prescribed and the common element boundary between element e and its adjacent elements. It's obvious that

$$\Gamma_e = \Gamma_{te} + \Gamma_{qe} + \Gamma_{ce} + \Gamma_{le} \qquad (15)$$
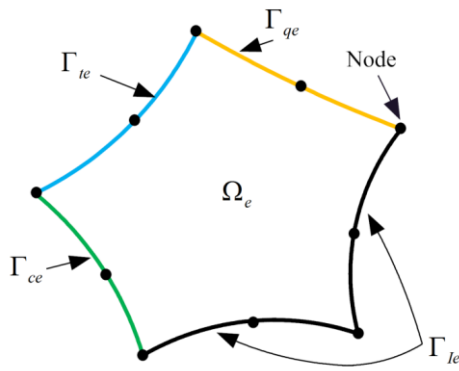
Figure 2. Illustration of a typical hybrid element

By invoking the divergence theorem

$$\int_{\Omega}\left(\frac{\partial f}{\partial X_1}\frac{\partial g}{\partial X_1}+\frac{\partial f}{\partial X_2}\frac{\partial g}{\partial X_2}\right)d\Omega = \int_{\Gamma}g\frac{\partial f}{\partial n}d\Gamma - \int_{\Omega}g\nabla^2 f d\Omega \quad (16)$$

for any smooth functions f and g in the domain, the first-order variation of Eq (14) is written as

$$\delta\Pi_{me} = \int_{\Omega_e}\left(K\nabla^2\Phi - S_b\Phi\right)\delta\Phi d\Omega + \int_{\Gamma_{te}}q\delta\tilde{\Phi}d\Gamma$$
$$+\int_{\Gamma_{qe}}\left(q-\bar{q}\right)\delta\tilde{\Phi}d\Gamma + \int_{\Gamma_{ce}}\left[q-H_\infty\left(\tilde{\Phi}-\Phi_\infty\right)\right]\delta\tilde{\Phi}d\Gamma \quad (17)$$
$$+\int_{\Gamma_e}\delta q\left(\tilde{\Phi}-\Phi\right)d\Gamma$$

from which it can be seen that the first, third and fourth integrals are associated with the governing equation (10), specified heat flux condition and convection condition in Eq. (12), respectively. The second integral will disappears when $\tilde{\Phi}$ is assumed to prior satisfy the specified temperature constraint on the boundary Γ_{te}. The last integral enforces the equality of Φ and $\tilde{\Phi}$ along the element frame Γ_e.

If the intra-element temperature satisfies the governing equation (10) analytically, then the hybrid functional (14) can be further simplified by applying the divergence theorem again to the functional (14), i.e.

$$\Pi_{me} = -\frac{1}{2}\int_{\Gamma_e}q\Phi d\Gamma + \int_{\Gamma_e}q\tilde{\Phi}d\Gamma$$
$$-\int_{\Gamma_{2e}}\bar{q}\tilde{\Phi}d\Gamma - \int_{\Gamma_{3e}}\frac{H_\infty}{2}\left(\tilde{\Phi}-\Phi_\infty\right)^2 d\Gamma \quad (18)$$

which inclulds boundary integrals only and can be used to derive the corresponding element stiffness equation.

2.3.2 Assumed Fields

To perform the HFS-FEM analysis, the solution domain Ω is divided into a number of elements. For a particular element, say element e, occupying a sub-domain Ω_e, with the element boundary Γ_e, two groups of independent fields Φ and $\tilde{\Phi}$ are assumed in the following way·

(1) Non-conforming intra-element fields

In the proposed fundamental-solution based hybrid finite element formulation, in order to construct the solution satisfying the governing equation (10) within the element domain, the temperature approximation Φ at any given point P within the element domain is expressed by a combination of fundamental solutions, as was done in the method of fundamental solutions (MFS) , for example,

$$\Phi = \sum_{i=1}^{n_s}G^*(P,Q_i)c_i = \mathbf{N}_e(P)\mathbf{c}_e, \quad P\in\Omega_e, Q_i\notin\Omega_e \quad (19)$$

where c_i is undetermined coefficients and n_s is the number of virtual sources Q_i surrounding the element domain. $G^*(P,Q_i)$ denotes the free-space Green's function (fundamental solutions) for the governing equation (10):

$$K\nabla^2 G^*(P,Q_i) - S_b G^*(P,Q_i) + \delta(P,Q_i) = 0 \quad (20)$$

whose solution is given by

$$G^*(P,Q_i) = -\frac{1}{2\pi K}K_0(\mu r) \quad (21)$$

In Eqs. (20) and (21), δ stands for the Dirac delta function, K_0 is the modified Bessel function of the second kind with order 0, $r = \|P-Q_i\|$ is the distance between the field point P and source point Q_i, and

$$\mu = \sqrt{\frac{S_b}{K}} \quad (22)$$

In the MFS, the coordinates of the source points Q_i are prescribed and usually they are chosen to locate on a pseudo boundary whose shape is similar to the element boundary Γ_e. Here, the locations of those source points

are determined by means of element nodes using the following relation [21]

$$x_{Q_i} = x_i + \gamma\left(x_i - x_c\right)$$
$$y_{Q_i} = y_i + \gamma\left(y_i - y_c\right)$$
(23)

where (x_{Q_i}, y_{Q_i}), (x_i, y_i) and (x_c, y_c) are respectively the coordinates of source point Q_i, nodal point i, and element center. The dimensionless parameter γ is used to control the distance of source points to the element physical boundary. It's obvious that the source points generated by Eq. (23) lie on a pseudo boundary similar to the element boundary.

Specially, in the absence of blood perfusion rate, the fundamental solutions used for intra-element approximation is given by

$$G^*(P, Q_i) = -\frac{1}{2\pi K}\ln(r)$$
(24)

Further, the heat flux is approximated by

$$q = -K\frac{\partial \Phi}{\partial n} = -K\sum_{i=1}^{n_s}\frac{\partial G^*(P, Q_i)}{\partial n}c_i = \mathbf{Q}_e\mathbf{c}_e$$
(25)

where

$$\frac{\partial G^*(P, Q_i)}{\partial n} = \frac{\mu}{2\pi K}K_1(\mu r)\frac{\partial r}{\partial n}$$
(26)

for the case of $\omega_b > 0$, and

$$\frac{\partial G^*(P, Q_i)}{\partial n} = -\frac{1}{2\pi K r}\frac{\partial r}{\partial n}$$
(27)

for the case of $\omega_b = 0$.

(2) Conforming frame fields defined on element boundary

An independent frame field defined over the element boundary can be approximated by the shape function interpolation widely used in the conventional FEM and BEM

$$\tilde{\Phi}(P) = \sum_{i=1}^{n_d}\tilde{N}_i(P)d_{ei} = \tilde{\mathbf{N}}_e(P)\mathbf{d}_e, \quad P \in \Gamma_e$$
(28)

where n_d is the number of nodes in the element, $\tilde{N}_i$ is the shape function.

The substitution of Eqs. (19), (25) and (28) into the functional (18) yields

$$\Pi_{me} = -\frac{1}{2}\mathbf{c}_e^{\mathrm{T}}\mathbf{H}_e\mathbf{c}_e - \mathbf{d}_e^{\mathrm{T}}\mathbf{g}_e + \mathbf{c}_e^{\mathrm{T}}\mathbf{G}_e\mathbf{d}_e - \frac{1}{2}\mathbf{d}_e^{\mathrm{T}}\mathbf{F}_e\mathbf{d}_e + \mathbf{d}_e^{\mathrm{T}}\mathbf{f}_e - \mathbf{a}_e$$

in which

$$\mathbf{H}_e = \int_{\Gamma_e}\mathbf{Q}_e^{\mathrm{T}}\mathbf{N}_e\mathrm{d}\Gamma, \quad \mathbf{G}_e = \int_{\Gamma_e}\mathbf{Q}_e^{\mathrm{T}}\tilde{\mathbf{N}}_e\mathrm{d}\Gamma,$$

$$\mathbf{g}_e = \int_{\Gamma_{eq}}\tilde{\mathbf{N}}_e^{\mathrm{T}}\overline{q}\mathrm{d}\Gamma, \quad \mathbf{F}_e = \int_{\Gamma_{ce}}h_\infty\tilde{\mathbf{N}}_e^{\mathrm{T}}\tilde{\mathbf{N}}_e\mathrm{d}\Gamma,$$

$$\mathbf{f}_e = \int_{\Gamma_{ce}}h_\infty T_\infty\tilde{\mathbf{N}}_e^{\mathrm{T}}\mathrm{d}\Gamma, \quad \mathbf{a}_e = \int_{\Gamma_{ce}}\frac{h_\infty T_\infty^2}{2}\mathrm{d}\Gamma$$

By virtue of the stationary conditions

$$\frac{\partial \Pi_{me}}{\partial \mathbf{c}_e^{\mathrm{T}}} = \mathbf{0}, \quad \frac{\partial \Pi_{me}}{\partial \mathbf{d}_e^{\mathrm{T}}} = \mathbf{0}$$

we obtain the following element stiffness equation for determining nodal temperature $\mathbf{d}_e$

$$\mathbf{K}_e\mathbf{d}_e = \mathbf{g}_e - \mathbf{f}_e$$
(29)

and the relationship of unknown coefficient $\mathbf{c}_e$ and $\mathbf{d}_e$

$$\mathbf{c}_e = \mathbf{H}_e^{-1}\mathbf{G}_e\mathbf{d}_e$$

In Eq. (29), the element stiffness matrix $\mathbf{K}_e$ has following form

$$\mathbf{K}_e = \mathbf{G}_e^{\mathrm{T}}\mathbf{H}_e^{-1}\mathbf{G}_e - \mathbf{F}_e$$

Assembling the element stiffness matrix element by element, we can obtain the global stiffness matrix, which still has the sparse and symmetrical features of the conventional finite element stiffness matrix.

III. Transient Heat Transfer in Skin Tissues

3.1 General mathematical equations

The bioheat transfer in a biological tissue can be described by the well-known Pennes equation in the following general form:

$$k^*\nabla^2 T^* + \rho_b^* c_b^* \omega_b^*\left(T_a^* - T^*\right) + Q_t^* = \rho^* c^*\frac{\partial T^*}{\partial t^*}$$
(30)

with the boundary conditions

$$\begin{cases} T^*(\mathbf{x}, t^*) = \overline{T}^*(\mathbf{x}, t^*) & \mathbf{x} \in \Gamma_1 \\ q^*(\mathbf{x}, t^*) = \overline{q}^*(\mathbf{x}, t^*) & \mathbf{x} \in \Gamma_2 \\ q^*(\mathbf{x}, t^*) = h_\infty^*(T^* - T_\infty^*) & \mathbf{x} \in \Gamma_3 \end{cases}$$
(31)

where ∇^2 represents the Laplacian operator, $T^*(\mathbf{x}, t^*)$ is the sought temperature field variable, t^* denotes time ($t^* > 0$). k^* is the thermal conductivity dependent on the special variables $\mathbf{x} \in \Omega$; ρ^* is the mass density and c is the specific heat. $Q_t^* = Q_m^* + Q_r^*$ stands for the general internal heat generation per unit volume due to metabolic heat and the laser beam. q^* represents the boundary normal heat flux defined by

$$q^* = -k^*\nabla T^* \cdot \mathbf{n} = -k^* \frac{\partial T^*}{\partial n} \quad (32)$$

n is the unit outward normal to the boundary Γ. A variable with over-bar denotes the variable being specified on given boundary. The constant T_a^* is artery temperature. The constant h_∞^* is the convection coefficient and T_∞^* is the environmental temperature. For a well-posed problem, we have $\Gamma = \Gamma_1 \cup \Gamma_2 \cup \Gamma_3$.

Finally, the initial condition is defined as

$$T^*(\mathbf{x}, t^* = 0) = T_0^*(x) \quad (33)$$

To avoid the potential numerical overflow of the present algorithm, the following dimensionless variables are employed in the analysis:

$$X = \frac{x}{L_0}, \qquad Y = \frac{y}{L_0}, \quad T = \frac{(T^* - T_a^*)k_0}{Q_0 L_0^2}, \quad k = \frac{k^*}{k_0}$$

$$\rho = \frac{\rho^*}{\rho_0}, \qquad c = \frac{c^*}{c_0}, \qquad t = \frac{t^* k_0}{L_0^2 \rho_0 c_0}, \qquad Q_t = \frac{Q_t^*}{Q_0} \quad (34)$$

where L_0 is the reference length of the biological body, k_0, ρ_0, c_0, and Q_0 are respectively reference values of the thermal conductivity, density, specific heat of tissue, and heat source term.

From Eq (34) we derive

$$\frac{\partial T^*}{\partial x} = \frac{Q_0 L_0^2}{k_0} \frac{1}{L_0} \frac{\partial T}{\partial X}, \qquad \frac{\partial T^*}{\partial y} = \frac{Q_0 L_0^2}{k_0} \frac{1}{L_0} \frac{\partial T}{\partial Y}$$

$$\frac{\partial^2 T^*}{\partial x^2} = \frac{Q_0 L_0^2}{k_0} \frac{1}{L_0^2} \frac{\partial^2 T}{\partial X^2}, \qquad \frac{\partial^2 T^*}{\partial y^2} = \frac{Q_0 L_0^2}{k_0} \frac{1}{L_0^2} \frac{\partial^2 T}{\partial Y^2} \quad (35)$$

$$\frac{\partial T^*}{\partial t^*} = \frac{Q_0 L_0^2}{k_0} \frac{k_0}{L_0^2 \rho_0 c_0} \frac{\partial T}{\partial t},$$

Substitution of Eq. (33) and Eq. (35) into Eq. (30) yields

$$k\nabla^2 T(\mathbf{x}, t) - \rho_b c_b \omega_b T(\mathbf{x}, t) + Q_t(\mathbf{x}) = \rho c \frac{\partial T(\mathbf{x}, t)}{\partial t} \quad (36)$$

where

$$\rho_b c_b \omega_b = \frac{\rho_b^* c_b^* \omega_b^* L_0^2}{k_0} \quad (37)$$

Correspondingly, the boundary conditions are rewritten as

$$\begin{cases} T(\mathbf{x}, t) = \overline{T}(\mathbf{x}, t) & \mathbf{x} \in \Gamma_1 \\ q(\mathbf{x}, t) = \overline{q}(\mathbf{x}, t) & \mathbf{x} \in \Gamma_2 \\ q(\mathbf{x}, t) = h_\infty(T - T_\infty) & \mathbf{x} \in \Gamma_3 \end{cases} \quad (38)$$

with

$$\overline{T} = \frac{(\overline{T}^* - T_a^*)k_0}{Q_0 L_0^2}, \quad \overline{q} = \frac{\overline{q}^*}{Q_0 L_0}, \quad h_\infty = \frac{h_\infty^* L_0}{k_0} \quad (39)$$

$$T_\infty = \frac{(T_\infty^* - T_a^*)k_0}{Q_0 L_0^2}, \quad q = -k \frac{\partial T}{\partial n}$$

3.2 Transient HFS-FEM Formulations

3.2.1 Direct Time Stepping

Making use of finite difference method, the derivative of temperature can be written as

$$\frac{\partial T(\mathbf{x}, t)}{\partial t} = \frac{T^{n+1}(\mathbf{x}) - T^n(\mathbf{x})}{\Delta t} \quad (40)$$

where Δt is the time-step, $T^{n+1}(\mathbf{x}) = T(\mathbf{x}, t^{n+1})$ and $T^n(\mathbf{x}) = T(\mathbf{x}, t^n)$ represent the temperature at the time instances t^{n+1} and t^n, respectively.

As a result, Eq. (36) at the time instance t^{n+1} can be rewritten as

$$k\nabla^2 T^{n+1}(\mathbf{x}) - \rho_b c_b \omega_b T^{n+1}(\mathbf{x}) + Q_t(\mathbf{x})$$
$$= \rho c \frac{T^{n+1}(\mathbf{x}) - T^n(\mathbf{x})}{\Delta t} \quad (41)$$

Rearranging Eq. (41) gives

$$\nabla^2 T^{n+1}(\mathbf{x}) - \lambda^2 T^{n+1}(\mathbf{x}) = b(\mathbf{x}) \quad (42)$$

with

$$\lambda = \sqrt{\frac{\rho c}{k \Delta t} + \frac{\rho_b c_b \omega_b}{k}} \quad (43)$$

$$b(\mathbf{x}) = -\frac{1}{k} Q_t(\mathbf{x}) - \frac{\rho c}{k \Delta t} T^n(\mathbf{x}) \quad (44)$$

Accordingly, the boundary conditions at time instance t^{n+1} can be represented as

$$\begin{cases} T^{n+1}(\mathbf{x}) = \overline{T}(\mathbf{x}, t^{n+1}) & \mathbf{x} \in \Gamma_1 \\ q^{n+1}(\mathbf{x}) = \overline{q}(\mathbf{x}, t^{n+1}) & \mathbf{x} \in \Gamma_2 \\ q^{n+1}(\mathbf{x}) = h_\infty(T^{n+1} - T_\infty) & \mathbf{x} \in \Gamma_3 \end{cases} \quad (45)$$

The linear system consisting of the governing partial differential equation (42) and boundary conditions (45)

is a standard inhomogeneous modified Helmholtz system, which will be solved by means of the present HFS-FEM and the dual reciprocity technique based on radial basis function interpolation described in the following sections.

3.2.2 Particular solution obtained using radial basis functions

Let T_p^{n+1} be a particular solution of the governing equation (42), we have

$$\nabla^2 T_p^{n+1}(\mathbf{x}) - \lambda^2 T_p^{n+1}(\mathbf{x}) = b(\mathbf{x}) \ (46)$$

but does not necessarily satisfy boundary condition (45).

Subsequently, the system consisting of Eq. (42) and Eq. (45) can be reduced to a homogeneous system by introducing two new variables as follows:

$$T_h^{n+1}(\mathbf{x}) = T^{n+1}(\mathbf{x}) - T_p^{n+1}(\mathbf{x})$$
$$q_h^{n+1}(\mathbf{x}) = q^{n+1}(\mathbf{x}) - q_p^{n+1}(\mathbf{x}) \ (47)$$

where

$$q_h^{n+1}(\mathbf{x}) = -k\frac{\partial T_h^{n+1}(\mathbf{x})}{\partial n}, \quad q_p^{n+1}(\mathbf{x}) = -k\frac{\partial T_p^{n+1}(\mathbf{x})}{\partial n} \ (48)$$

Substituting Eq. (47) into Eq. (42), we obtain the following homogeneous equation

$$\nabla^2 T_h^{n+1}(\mathbf{x}) - \lambda^2 T_h^{n+1}(\mathbf{x}) = 0 \ (49)$$

with modified boundary conditions

$$\begin{cases} T_h^{n+1}(\mathbf{x}) = \bar{T}_h(\mathbf{x}) = \bar{T}(\mathbf{x}, t^{n+1}) - T_p^{n+1}(\mathbf{x}) & \mathbf{x} \in \Gamma_1 \\ q_h^{n+1}(\mathbf{x}) = \bar{q}_h(\mathbf{x}) = \bar{q}(\mathbf{x}, t^{n+1}) - q_p^{n+1}(\mathbf{x}) & \mathbf{x} \in \Gamma_2 \\ q_h^{n+1}(\mathbf{x}) = h_\infty\left\{T_h^{n+1}(\mathbf{x}) - T_\infty^{n+1}(\mathbf{x})\right\} & \mathbf{x} \in \Gamma_3 \end{cases} \ (50)$$

where

$$T_\infty^{n+1}(\mathbf{x}) = -T_p^{n+1}(\mathbf{x}) + T_\infty + \frac{q_p^{n+1}(\mathbf{x})}{h_\infty} \ (51)$$

The above homogeneous system can be solved using the hybrid finite element model described in the next section.

The above homogeneous system can be solved using the hybrid finite element model described in the next section.

In what follows, we describe the solution procedure for the particular solution part $T_p^{n+1}(\mathbf{x})$. For the arbitrary right-handed source term $b(\mathbf{x})$, the particular solution $T_p^{n+1}(\mathbf{x})$ can be determined numerically by the dual reciprocity technique, in which it is essential to approximate the source term by a series of basic

functions, i.e. radial basis functions (RBFs).

Let ϕ be a radial basis function. Then the source term $b(\mathbf{x})$ in Eq. (46) can be approximated as follows[26]

$$b(\mathbf{x}) = \sum_{j=1}^{M} \alpha_j \phi(r_j) \ (52)$$

where $r_j = \|\mathbf{x} - \mathbf{x}_j\|$ denotes the Euclidean distance between the field point $\mathbf{x}$ and source point $\mathbf{x}_j$, and α_j are unknown coefficients.

Making use of Eq. (52), the particular solution can be obtained as

$$T_p^{n+1}(\mathbf{x}) = \sum_{j=1}^{M} \alpha_j \Phi(r_j) \ (53)$$

where the function is governed by

$$\nabla^2 \Phi(r_j) - \lambda^2 \Phi(r_j) = \phi(r_j) \ (54)$$

Taking the thin plate spline (TPS)

$$\phi(r_j) = r_j^2 \ln(r_j) \ (55)$$

as an example, the approximate particular solution can be obtained by the annihilator method as[105]

$$\Phi(r_j) = \begin{cases} -\dfrac{4}{\lambda^4} - \dfrac{4}{\lambda^4}\ln r_j - \dfrac{1}{\lambda^2} r_j^2 \ln r_j \\ \\ -\dfrac{4}{\lambda^4} K_0\left(\lambda r_j\right), \qquad\qquad r_j \neq 0 \ (56) \\ \\ -\dfrac{4}{\lambda^4} + \dfrac{4\gamma}{\lambda^4} + \dfrac{4}{\lambda^4}\ln\left(\dfrac{\lambda}{2}\right), \qquad r_j = 0 \end{cases}$$

where $=0.5772156649015328$ is Euler's constant.

3.2.3 Homogeneous Solution Using the Hybrid Finite Element Model

To perform the hybrid finite element analysis in a convenient way, the boundary conditions given in Eq. (50) are rewritten as

$$\begin{cases} T_h^{n+1}(\mathbf{x}) = \bar{T}_h(\mathbf{x}) & \mathbf{x} \in \Gamma_1 \\ \chi_h^{n+1}(\mathbf{x}) = \bar{\chi}_h(\mathbf{x}) & \mathbf{x} \in \Gamma_2 \ (57) \\ \chi_h^{n+1}(\mathbf{x}) = \bar{h}_\infty\left\{T_h^{n+1}(\mathbf{x}) - T_\infty^{n+1}(\mathbf{x})\right\} & \mathbf{x} \in \Gamma_3 \end{cases}$$

with

$$\chi_h^{n+1}(\mathbf{x}) = \frac{\partial T_h^{n+1}(\mathbf{x})}{\partial n}, \quad \bar{\chi}_h(\mathbf{x}) = -\bar{q}_h(\mathbf{x})/k, \quad \bar{h}_\infty = -\frac{h_\infty}{k} \ (58)$$

Then, the following hybrid variational functional expressed at element level can be constructed as

$$\Pi_{me} = \frac{1}{2}\int_{\Omega_e}\left(T_{,i}T_{,i} + \lambda^2 T^2\right)d\Omega - \int_{\Gamma_{2e}}\bar{\chi}\tilde{T}d\Gamma$$
$$+\int_{\Gamma_e}\chi\left(\tilde{T}-T\right)d\Gamma - \frac{1}{2}\int_{\Gamma_{3e}}\bar{h}_\infty\left(\tilde{T}-T_\infty\right)^2 d\Gamma \quad (59)$$

in which T is the temperature field defined inside the element domain Ω_e with the boundary Γ_e, $\tilde{T}$ denotes the frame field defined along the element boundary, and $\Gamma_{2e} = \Gamma_2 \cap \Gamma_e$, $\Gamma_{3e} = \Gamma_3 \cap \Gamma_e$. Note that in Eq. (59), the superscript 'n+1' and subscript 'h' are discarded for the sake of simplicity.

By invoking the divergence theorem and assuming that $\tilde{T}$ satisfies the specified temperature boundary condition (the first equation of Eq. (57)) and the compatibility condition on the interface between the element under consideration and its adjacent elements as prerequisites, variation of Eq. (59) can be written as

$$\delta\Pi_{me} = -\int_{\Omega_e}\left(T_{,ii} - \lambda^2 T\right)\delta T d\Omega + \int_{\Gamma_{2e}}\left(\chi - \bar{\chi}\right)\delta\tilde{T}d\Gamma$$
$$+\int_{\Gamma_e}\delta\chi\left(\tilde{T}-T\right)d\Gamma + \int_{\Gamma_{3e}}\left[\chi - \bar{h}_\infty\left(\tilde{T}-T_\infty\right)\right]\delta\tilde{T}d\Gamma \quad (60)$$

from which it can be seen that the third integral enforces the equality of T and $\tilde{T}$ along the element boundary Γ_e. The first, second and fourth integrals enforce respectively the governing equation (49), flux, and convection boundary conditions (the second and third equations in (57)).

If the internal temperature field T satisfies the homogeneous modified Helmholtz equation, i.e.
$$\nabla^2 T - \lambda^2 T = 0 \quad (61)$$
then applying the divergence theorem again to the functional (59), we have

$$\Pi_{me} = -\frac{1}{2}\int_{\Gamma_e}\chi T d\Gamma - \int_{\Gamma_{2e}}\bar{\chi}\tilde{T}d\Gamma$$
$$+\int_{\Gamma_e}\chi\tilde{T}d\Gamma - \int_{\Gamma_{3e}}\frac{\bar{h}_\infty}{2}\left(\tilde{T}-T_\infty\right)^2 d\Gamma \quad (62)$$

In the proposed HFS-FEM, the variable T is given as a superposition of fundamental solutions $G^*(P,Q_j)$ at n_s source points to guarantee the satisfaction of Eq. (60)

$$T_h^{n+1} = \sum_{j=1}^{n_s}G^*(P,Q_j)c_{ej} = \mathbf{N}_e(P)\mathbf{c}_e, \quad P \in \Omega_e, Q_j \notin \Omega_e \quad (63)$$

where c_{ej} is undetermined coefficients and n_s is the number of virtual sources Q_j applied at points outside

the element.

The free-space fundamental solution of the modified Helmholtz operator can be obtained as the solution of
$$\nabla^2 G^*(P,Q_j) - \lambda^2 G^*(P,Q_j) = -\delta(P,Q_j) \quad (64)$$
and is given by[106]
$$G^*(P,Q_j) = -\frac{1}{2\pi}K_0(\lambda\|P-Q_j\|) \quad (65)$$

where $\delta(P,Q_j)$ is the Dirac delta function and K_0 denotes the modified Bessel function of the second kind with order 0.

Simultaneously, the independent frame variable on the element boundary can be defined by the standard shape function interpolation

$$\tilde{T}(P) = \sum_{i=1}^{n}\tilde{N}_i(P)d_{ei} = \tilde{\mathbf{N}}_e(P)\mathbf{d}_e, \quad P \in \Gamma_e \quad (66)$$

where n is the number of nodes of the element under consideration, $\tilde{N}_i$ is the shape function and d_{ei} is nodal temperature. Their descriptions can be found in standard finite element texts and are not repeated here.

By substitution of Eq. (63) and Eq. (66) into Eq. (62) we obtain

$$\Pi_{me} = -\frac{1}{2}\mathbf{c}_e^T\mathbf{H}_e\mathbf{c}_e - \mathbf{d}_e^T\mathbf{g}_e + \mathbf{c}_e^T\mathbf{G}_e\mathbf{d}_e$$
$$-\frac{1}{2}\mathbf{d}_e^T\mathbf{F}_e\mathbf{d}_e + \mathbf{d}_e^T\mathbf{f}_e - \mathbf{a}_e \quad (67)$$

in which
$$\mathbf{H}_e = \int_{\Gamma_e}\mathbf{Q}_e^T\mathbf{N}_e d\Gamma, \quad \mathbf{G}_e = \int_{\Gamma_e}\mathbf{Q}_e^T\tilde{\mathbf{N}}_e d\Gamma,$$
$$\mathbf{g}_e = \int_{\Gamma_{2e}}\tilde{\mathbf{N}}_e^T\bar{q}d\Gamma, \quad \mathbf{F}_e = \int_{\Gamma_{3e}}\bar{h}_\infty\tilde{\mathbf{N}}_e^T\tilde{\mathbf{N}}_e d\Gamma, \quad (68)$$
$$\mathbf{f}_e = \int_{\Gamma_{3e}}\bar{h}_\infty T_\infty\tilde{\mathbf{N}}_e^T d\Gamma, \quad \mathbf{a}_e = \int_{\Gamma_{3e}}\frac{\bar{h}_\infty T_\infty^2}{2}d\Gamma$$

and
$$\mathbf{Q}_e = \frac{\partial\mathbf{N}_e}{\partial n} \quad (69)$$

IV. CONCLUSION

1) On the basis of the preceding discussion, the following conclusions can be drawn. This review reports recent developments on applications of hybrid F-Trefftz finite element method to skin tissues and structures. It proved to be a powerful

computational tool in modeling materials and structures with various mechanical properties. However, there are still many possible extensions and areas in need of further development in the future. Among those developments one could list the following:

2) Development of efficient F-Trefftz FE-BEM schemes for complex engineering structures containing heterogeneous materials and the related general purpose computer codes with preprocessing and postprocessing capabilities.

3) Generation of various special-purpose elements to effectively handle singularities attributable to local geometrical or load effects (holes, cracks, inclusions, interface, corner and load singularities). The special-purpose functions warrant that excellent results are obtained at minimal computational cost and without local mesh refinement.

4) Development of F-Trefftz FE in conjunction with a topology optimization scheme to contribute to microstructure design.

5) Extension of the F-Trefftz FEM to elastodynamics and fracture mechanics of FGMs.

V. REFERENCES

[1] H. Wang, W. Zhang, Q.H. Qin, Numerical simulation of thermal properties in 2D biological tissue using the method of fundamental solution, in: Recent Studies in Meshless Methods (ed. By Z.H. Yao, J. Soric, S. N. Atluri), Proceedings of the 4th ICCES Meshless and other novel computational methods, Suzhou, China, Tech Science Press, Norcross, Tech Science Press, 2009, pp. 25-42.

[2] H. Wang, Q.H. Qin, M.Y. Han, Hybrid finite element simulation for bioheat transfer in the human eye, in: Ophthalmological Imaging and Applications, CRC Press, 2014, pp. 409-425.

[3] Z.-W. Zhang, H. Wang, Q.H. Qin, Meshless Method with Operator Splitting Technique for Transient Nonlinear Bioheat Transfer in Two-Dimensional Skin Tissues, International Journal of Molecular Sciences, 16(1) (2015) 2001-2019.

[4] L.-L. Cao, Q.H. Qin, N. Zhao, A new RBF-Trefftz meshless method for partial differential equations, IOP Conference Series: Materials Science and Engineering, 10 (2010) 012217.

[5] Q.H. Qin, Y.W. Mai, A closed crack tip model for interface cracks in thermopiezoelectric materials, International Journal of Solids and Structures, 36(16) (1999) 2463-2479.

[6] S.W. Yu, Q.H. Qin, Damage analysis of thermopiezoelectric properties: Part II. Effective crack model, Theoretical and Applied Fracture Mechanics, 25(3) (1996) 279-288.

[7] Q.H. Qin, 2D Green's functions of defective magnetoelectroelastic solids under thermal loading, Engineering Analysis with Boundary Elements, 29(6) (2005) 577-585.

[8] Q.H. Qin, General solutions for thermopiezoelectrics with various holes under thermal loading, International Journal of Solids and Structures, 37(39) (2000) 5561-5578.

[9] Q.H. Qin, Green's function and boundary elements of multifield materials, Elsevier, Oxford, 2007.

[10] Q.H. Qin, Y.W. Mai, S.W. Yu, Some problems in plane thermopiezoelectric materials with holes, International Journal of Solids and Structures, 36(3) (1999) 427-439.

[11] Q.H. Qin, Y.W. Mai, Crack growth prediction of an inclined crack in a half-plane thermopiezoelectric solid, Theoretical and Applied Fracture Mechanics, 26(3) (1997) 185-191.

[12] Q.H. Qin, Fracture mechanics of piezoelectric materials, WIT Press, Southampton, 2001.

[13] Q.H. Qin, S.W. Yu, An arbitrarily-oriented plane crack terminating at the interface between dissimilar piezoelectric materials, International Journal of Solids and Structures, 34(5) (1997) 581-590.

[14] S.W. Yu, Q.H. Qin, Damage analysis of thermopiezoelectric properties: Part I—crack tip singularities, Theoretical and Applied Fracture Mechanics, 25(3) (1996) 263-277.

[15] J.S. Wang, G.F. Wang, X.Q. Feng, Q.H. Qin, Surface effects on the superelasticity of nanohelices, Journal of Physics: Condensed Matter, 24(26) (2012) 265303.

[16] J.S. Wang, X.Q. Feng, J. Xu, Q.H. Qin, S.W. Yu, Chirality transfer from molecular to morphological scales in quasi-one-dimensional nanomaterials: a continuum model, Journal of Computational and Theoretical Nanoscience, 8(7) (2011) 1278-1287.

[17] J.-S. Wang, G.-F. Wang, X.-Q. Feng, Q.-H. Qin, Surface effects on the superelasticity of

nanohelices, Journal of Physics: Condensed Matter, 24(26) (2012) 265303.

[18] H. Wang, Q.H. Qin, Y. Xiao, Special n-sided Voronoi fiber/matrix elements for clustering thermal effect in natural-hemp-fiber-filled cement composites, International Journal of Heat and Mass Transfer, 92 (2016) 228-235.

[19] Q.H. Qin, The Trefftz finite and boundary element method, WIT Press, Southampton, 2000.

[20] Q.H. Qin, Trefftz finite element method and its applications, Applied Mechanics Reviews, 58(5) (2005) 316-337.

[21] H. Wang, Q.H. Qin, Y. Kang, A meshless model for transient heat conduction in functionally graded materials, Computational Mechanics, 38(1) (2006) 51-60.

[22] N. Bavi, Q.H. Qin, B. Martinac, Finite element simulation of the gating mechanism of mechanosensitive ion channels, in: Fourth International Conference on Smart Materials and Nanotechnology in Engineering, International Society for Optics and Photonics, 2013, pp. 87931S-87931S-87937.

[23] C. Liu, Y. Zhang, Q.H. Qin, R.B. Heslehurst, Numerical Modelling of Glass Fibre Metal Laminates Subjected to High Velocity Impact, in: Proceedings of the Composites Australia and CRC-ACS, 2013 Composites Conference (Edited by Rikard Heslehurst), Melbourne, 4-5 March 2013, 2013.

[24] C.J. Liu, Y. Zhang, Q.H. Qin, R. Heslehurst, High velocity impact modelling of sandwich panels with aluminium foam core and aluminium sheet skins, in: Applied Mechanics and Materials, 2014, pp. 745-750.

[25] Z.-J. Fu, Q.H. Qin, W. Chen, Hybrid-Trefftz finite element method for heat conduction in nonlinear functionally graded materials, Engineering Computations, 28(5) (2011) 578-599.

[26] Q.H. Qin, H. Wang, Matlab and C programming for Trefftz finite element methods, New York: CRC Press, 2008.

[27] Q.H. Qin, C.X. Mao, Coupled torsional-flexural vibration of shaft systems in mechanical engineering—I. Finite element model, Computers & Structures, 58(4) (1996) 835-843.

[28] H.C. Martin, G.F. Carey, Introduction to finite element analysis: Theory and application, McGraw-Hill New York, 1973.

[29] H. Wang, Y. Xiao, Q.H. Qin, 2D hierarchical heat transfer computational model of natural ber bundle reinforced composite, Scientia Iranica, Transactions B: Mechanical Engineering, 23(1) (2016) 268-276.

[30] K.Z. Ding, Q.H. Qin, M. Cardew-Hall, A New Integration Algorithm for the Finite Element Analysis of Elastic-Plastic Problems, in: Proc. of 9th International Conference on Inspection, Appraisal, Repairs & Maintenance of Structures, Fuzhou, China, 20-21 October, CI-Premier PTY LTD, ISBN: 981-05-3548-1, 2005, pp. 209-216.

[31] Q.H. Qin, Y.W. Mai, BEM for crack-hole problems in thermopiezoelectric materials, Engineering Fracture Mechanics, 69(5) (2002) 577-588.

[32] Q.H. Qin, Y. Huang, BEM of postbuckling analysis of thin plates, Applied Mathematical Modelling, 14(10) (1990) 544-548.

[33] Q.H. Qin, Nonlinear analysis of Reissner plates on an elastic foundation by the BEM, International journal of solids and structures, 30(22) (1993) 3101-3111.

[34] W. Chen, Z.-J. Fu, Q.-H. Qin, Boundary particle method with high-order Trefftz functions, Computers, Materials & Continua (CMC), 13(3) (2010) 201-217.

[35] H. Wang, Q.H. Qin, D. Arounsavat, Application of hybrid Trefftz finite element method to non‐linear problems of minimal surface, International Journal for Numerical Methods in Engineering, 69(6) (2007) 1262-1277.

[36] H. Wang, Q.-H. Qin, X.-P. Liang, Solving the nonlinear Poisson-type problems with F-Trefftz hybrid finite element model, Engineering Analysis with Boundary Elements, 36(1) (2012) 39-46.

[37] Q.H. Qin, Dual variational formulation for Trefftz finite element method of elastic materials, Mechanics Research Communications, 31(3) (2004) 321-330.

[38] H. Wang, Q.-H. Qin, Numerical implementation of local effects due to two-dimensional discontinuous loads using special elements based on boundary integrals, Engineering Analysis with Boundary Elements, 36(12) (2012) 1733-1745.

[39] Q.H. Qin, Formulation of hybrid Trefftz finite element method for elastoplasticity, Applied Mathematical Modelling, 29(3) (2005) 235-252.

[40] Q.-H. Qin, Trefftz plane elements of elastoplasticity with p-extension capabilities, Journal of Mechanical Engineering, 56(1) (2005) 40-59.

[41] Y. Cui, Q.H. Qin, Fracture analysis of mode III problems by Trefftz finite element approach, in: WCCM VI in conjunction with APCOM, 2004, pp. v1-p380.

[42] Y.-h. Cui, Q.H. Qin, J.-S. Wang, Application of HT finite element method to multiple crack problems of Mode I, II and III, Chinese Journal of Engineering Mechanics, 23(3) (2006) 104-110.

[43] Y. Cui, J. Wang, M. Dhanasek, Q.H. Qin, Mode III fracture analysis by Trefftz boundary element method, Acta Mechanica Sinica, 23(2) (2007) 173-181.

[44] C. Cao, Q.H. Qin, A. Yu, Micromechanical Analysis of Heterogeneous Composites using Hybrid Trefftz FEM and Hybrid Fundamental Solution Based FEM, Journal of Mechanics, 29(4) (2013) 661-674.

[45] C. Cao, A. Yu, Q.H. Qin, Evaluation of effective thermal conductivity of fiber-reinforced composites by boundary integral based finite element method, International Journal of Architecture, Engineering and Construction, 1(1) (2012) 14-29.

[46] M. Dhanasekar, J. Han, Q.H. Qin, A hybrid-Trefftz element containing an elliptic hole, Finite Elements in Analysis and Design, 42(14) (2006) 1314-1323.

[47] Q.H. Qin, X.-Q. He, Special elliptic hole elements of Trefftz FEM in stress concentration analysis, Journal of Mechanics and MEMS, 1(2) (2009) 335-348.

[48] J. Jirousek, Q.H. Qin, Application of hybrid-Trefftz element approach to transient heat conduction analysis, Computers & Structures, 58(1) (1996) 195-201.

[49] L. Cao, Q.H. Qin, N. Zhao, Application of DRM-Trefftz and DRM-MFS to Transient Heat Conduction Analysis, Recent Patents on Space Technology (Open access), 2 (2010) 41-50.

[50] N. Zhao, L.-L. Cao, Q.-H. Qin, Application of Trefftz Method to Heat Conduction Problem in Functionally Graded Materials, Recent Patents on Space Technology, 1(2) (2011) 158-166.

[51] Q.H. Qin, Hybrid Trefftz finite-element approach for plate bending on an elastic foundation, Applied Mathematical Modelling, 18(6) (1994) 334-339.

[52] Q.H. Qin, Postbuckling analysis of thin plates by a hybrid Trefftz finite element method, Computer Methods in Applied Mechanics and Engineering, 128(1) (1995) 123-136.

[53] Q.H. Qin, Transient plate bending analysis by hybrid Trefftz element approach, Communications in Numerical Methods in Engineering, 12(10) (1996) 609-616.

[54] Q.H. Qin, Postbuckling analysis of thin plates on an elastic foundation by HT FE approach, Applied Mathematical Modelling, 21(9) (1997) 547-556.

[55] F. Jin, Q.H. Qin, A variational principle and hybrid Trefftz finite element for the analysis of Reissner plates, Computers & Structures, 56(4) (1995) 697-701.

[56] J. Jirousek, A. Wroblewski, Q.H. Qin, X. He, A family of quadrilateral hybrid-Trefftz p-elements for thick plate analysis, Computer Methods in Applied Mechanics and Engineering, 127(1) (1995) 315-344.

[57] Q.H. Qin, Hybrid-Trefftz Finite-Element Method for Reissner Plates on an Elastic-Foundation, Computer Methods in Applied Mechanics and Engineering, 122(3-4) (1995) 379-392.

[58] Q.H. Qin, S. Diao, Nonlinear analysis of thick plates on an elastic foundation by HT FE with p-extension capabilities, International Journal of Solids and Structures, 33(30) (1996) 4583-4604.

[59] Q.H. Qin, Nonlinear analysis of thick plates by HT FE approach, Computers & Structures, 61(2) (1996) 271-281.

[60] C.-Y. Lee, Q.H. Qin, H. Wang, Trefftz functions and application to 3D elasticity, Computer Assisted Mechanics and Engineering Sciences, 15 (2008) 251-263.

[61] Q.H. Qin, Variational formulations for TFEM of piezoelectricity, International Journal of Solids and Structures, 40(23) (2003) 6335-6346.

[62] Q.H. Qin, Solving anti-plane problems of piezoelectric materials by the Trefftz finite element approach, Computational Mechanics, 31(6) (2003) 461-468.

[63] Q.H. Qin, Mode III fracture analysis of piezoelectric materials by Trefftz BEM, Structural Engineering and Mechanics, 20(2) (2005) 225-240.

[64] Q.H. Qin, Fracture Analysis of Piezoelectric Materials by Boundary and Trefftz Finite Element Methods, WCCM VI in conjunction with APCOM'04, Sept. 5-10, 2004, Beijing, China, (2004).

[65] Q.H. Qin, Trefftz Plane Element of Piezoelectric Plate with p-Extension Capabilities, IUTAM Symposium on Mechanics and Reliability of Actuating Materials, (2006) 144-153.

[66] Q.H. Qin, K.-Y. Wang, Application of hybrid-Trefftz finite element method fractional contact problems, Computer Assisted Mechanics and Engineering Sciences, 15 (2008) 319-336.

[67] K. Wang, Q.H. Qin, Y. Kang, J. Wang, C. Qu, A direct constraint‐Trefftz FEM for analysing elastic contact problems, International Journal for Numerical Methods in Engineering, 63(12) (2005) 1694-1718.

[68] M. Dhanasekar, K.Y. Wang, Q.H. Qin, Y.L. Kang, Contact analysis using Trefftz and interface finite elements, Computer Assisted Mechanics and Engineering Sciences, 13(3) (2006) 457-471.

[69] H. Wang, Q.H. Qin, Hybrid FEM with fundamental solutions as trial functions for heat conduction simulation, Acta Mechanica Solida Sinica, 22(5) (2009) 487-498.

[70] C. Cao, Q.-H. Qin, Hybrid fundamental solution based finite element method: theory and applications, Advances in Mathematical Physics, 2015 (2015).

[71] Q.H. Qin, Fundamental Solution Based Finite Element Method, J Appl Mech Eng, 2 (2013) e118.

[72] Z.-J. Fu, W. Chen, Q.H. Qin, Hybrid Finite Element Method Based on Novel General Solutions for Helmholtz-Type Problems, Computers Materials and Continua, 21(3) (2011) 187.

[73] Y.-T. Gao, H. Wang, Q.-H. Qin, Orthotropic Seepage Analysis using Hybrid Finite Element Method, Journal of Advanced Mechanical Engineering, 2(1) (2015) 1-13.

[74] H. Wang, Q.H. Qin, Fundamental solution-based hybrid finite element analysis for non-linear minimal surface problems, Recent Developments in Boundary Element Methods: A Volume to Honour Professor John T. Katsikadelis, 309 (2010).

[75] H. Wang, Q.-H. Qin, Fundamental-solution-based hybrid FEM for plane elasticity with special elements, Computational Mechanics, 48(5) (2011) 515-528.

[76] H. Wang, Q.H. Qin, W. Yao, Improving accuracy of opening-mode stress intensity factor in two-dimensional media using fundamental solution based finite element model, Australian Journal of Mechanical Engineering, 10(1) (2012) 41-51.

[77] Q.H. Qin, H. Wang, Special Elements for Composites Containing Hexagonal and Circular Fibers, International Journal of Computational Methods, 12(04) (2015) 1540012.

[78] H. Wang, Q.H. Qin, Special fiber elements for thermal analysis of fiber-reinforced composites, Engineering Computations, 28(8) (2011) 1079-1097.

[79] H. Wang, Q.H. Qin, A fundamental solution based FE model for thermal analysis of nanocomposites, in: Boundary elements and other mesh Reduction methods XXXIII', 33rd International Conference on Boundary Elements and other Mesh Reduction Methods, ed. CA Brebbia and V. Popov, WIT Press, UK, 2011, pp. 191-202.

[80] H. Wang, Q.H. Qin, Implementation of fundamental-solution based hybrid finite element model for elastic circular inclusions, in: Proceedings of the Asia-Pacific Congress for Computational Mechanics, 11th-14th Dec, 2013.

[81] C. Cao, Q.H. Qin, A. Yu, Modelling of Anisotropic Composites by Newly Developed HFS-FEM, in: Proceedings of the 23rd International Congress of Theoretical and Applied Mechanics, Yilong Bai , Jianxiang Wang , Daining Fang (eds), SM08-016, August 19 - 24 , 2012, Beijing, China, The International Union of Theoretical and Applied Mechanics (IUTAM), 2012.

[82] C. Cao, Q.H. Qin, A. Yu, Hybrid fundamental-solution-based FEM for piezoelectric materials, Computational Mechanics, 50(4) (2012) 397-412.

[83] C. Cao, A. Yu, Q.-H. Qin, A new hybrid finite element approach for plane piezoelectricity with defects, Acta Mechanica, 224(1) (2013) 41-61.

[84] H. Wang, Q.H. Qin, Fracture analysis in plane piezoelectric media using hybrid finite element model, in: International Conference of fracture, 2013.

[85] C. Cao, Q.-H. Qin, A. Yu, A new hybrid finite element approach for three-dimensional elastic problems, Archives of Mechanics, 64(3) (2012) 261-292.

[86] L.-L. Cao, Q.-H. Qin, N. Zhao, Hybrid graded element model for transient heat conduction in functionally graded materials, Acta Mechanica Sinica, 28(1) (2012) 128-139.

[87] L. Cao, H. Wang, Q.-H. Qin, Fundamental solution based graded element model for steady-state heat transfer in FGM, Acta Mechanica Solida Sinica, 25(4) (2012) 377-392.

[88] H. Wang, Q.-H. Qin, Boundary integral based graded element for elastic analysis of 2D functionally graded plates, European Journal of Mechanics-A/Solids, 33 (2012) 12-23.

[89] H. Wang, Q.H. Qin, FE approach with Green's function as internal trial function for simulating bioheat transfer in the human eye, Archives of Mechanics, 62(6) (2010) 493-510.

[90] H. Wang, Q.H. Qin, Computational bioheat modeling in human eye with local blood perfusion effect, Human Eye Imaging and Modeling, (2012).

[91] H. Wang, Q.-H. Qin, A fundamental solution-based finite element model for analyzing multi-layer skin burn injury, Journal of Mechanics in Medicine and Biology, 12(05) (2012) 1250027.

[92] Z.-W. Zhang, H. Wang, Q.-H. Qin, Transient bioheat simulation of the laser-tissue interaction in human skin using hybrid finite element formulation, Molecular & Cellular Biomechanics, 9(1) (2012) 31-53.

[93] Z.W. Zhang, H. Wang, Q.H. Qin, Analysis of transient bioheat transfer in the human eye using hybrid finite element model, in: Applied Mechanics and Materials, Trans Tech Publ, 2014, pp. 356-361.

[94] J. Tao, Q.H. Qin, L. Cao, A Combination of Laplace Transform and Meshless Method for Analysing Thermal Behaviour of Skin Tissues, Universal Journal of Mechanical Engineering, 1(2) (2013) 32-42.

[95] Z.W. Zhang, H. Wang, Q.H. Qin, Method of fundamental solutions for nonlinear skin bioheat model, Journal of Mechanics in Medicine and Biology, 14(4) (2014) 1450060.

[96] C. Cao, Q.-H. Qin, A. Yu, A novel boundary-integral based finite element method for 2D and 3D thermo-elasticity problems, Journal of Thermal Stresses, 35(10) (2012) 849-876.

[97] Q.H. Qin, H. Wang, Special circular hole elements for thermal analysis in cellular solids with multiple circular holes, International Journal of Computational Methods, 10(04) (2013) 1350008.

[98] H. Wang, Q.-H. Qin, A new special element for stress concentration analysis of a plate with elliptical holes, Acta Mechanica, 223(6) (2012) 1323-1340.

[99] Q.H. Qin, H. Wang, Fundamental solution based FEM for nonlinear thermal radiation problem, in: 12th International Conference on Boundary Element and Meshless Techniques (BeTeq 2011), ed. EL Albuquerque, MH Aliabadi, EC Ltd, Eastleigh, UK, 2011, pp. 113-118.

[100] C. Cao, A. Yu, Q.-H. Qin, A novel hybrid finite element model for modeling anisotropic composites, Finite Elements in Analysis and Design, 64 (2013) 36-47.

[101] C. Cao, A. Yu, Q.H. Qin, Mesh reduction strategy: Special element for modelling anisotropic materials with defects, Boundary Elements and Other Mesh Reduction Methods XXXVI, 56 (2013) 61.

[102] H. Wang, Q.-H. Qin, Fundamental-solution-based finite element model for plane orthotropic elastic bodies, European Journal of Mechanics-A/Solids, 29(5) (2010) 801-809.

[103] S. Jiang, N. Ma, H. Li, X. Zhang, Effects of thermal properties and geometrical dimensions on skin burn injuries, Burns, 28(8) (2002) 713-717.

[104] E. Ng, H. Tan, E. Ooi, Boundary element method with bioheat equation for skin burn injury, Burns, 35(7) (2009) 987-997.

[105] A. Muleshkov, M. Golberg, C. Chen, Particular solutions of Helmholtz-type operators using higher order polyhrmonic splines, Computational Mechanics, 23(5-6) (1999) 411-419.

[106] K. Balakrishnan, P. Ramachandran, The method of fundamental solutions for linear diffusion-reaction equations, Mathematical and Computer Modelling, 31(2) (2000) 221-237.